Journal of Thermal Analysis and Calorimetry, Vol. 92 (2008) 3, 931–937

THE PHASE DIAGRAM OF V_2O_5–MoO_3–Ag_2O SYSTEM
Part IV. Molybdenum-rich part of the diagram

E. Wenda[1]* *and A. Bielański*[1, 2]

[1]Faculty of Chemistry, Jagiellonian University, ul. R. Ingardena 3, 30-060 Cracow, Poland
[2]Polish Academy of Sciences, Institute of Catalysis and Surface Chemistry, ul. Niezapominajek 8, 30-239 Cracow, Poland

The results concerning the synthesis, structure and thermal properties of V_2O_5–MoO_3–Ag_2O samples in the molybdenum rich region of ternary system are presented in the form of quasi-binary systems: β–$AgVO_3$–β-Ag_2MoO_4, $AgVMoO_6$–MoO_3, $AgVMoO_6$–$Ag_2Mo_4O_{13}$, $AgVMoO_6$–$Ag_2Mo_2O_7$, $AgVMoO_6$–β-Ag_2MoO_4 and also of the system in which at V_2O_5/MoO_3 molar ratio 3:7 the content of Ag_2O was variable. The ternary phase $AgVMoO_6$ was not described earlier in the literature.

Keywords: *molybdena, phase diagram, silver oxide, vanadia*

Introduction

In the previous publication of this series the sections of the ternary diagram V_2O_5–MoO_3–Ag_2O in its vanadium rich region were presented in which at vanadia/molybdena molar ratios 9:1, 7:3 and 1:1 different amounts of Ag_2O were introduced [1]. Generally the phases which were identified in the V_2O_5–MoO_3–Ag_2O system in this region corresponded then to the phases observed in the binary V_2O_5–Ag_2O system beside which $AgVMoO_6$ phase appeared. Liquidus line of V_2O_5-phase in V_2O_5–Ag_2O binary system turns into crystallisation surface in ternary diagram, liquidus line of β-bronze in V_2O_5–Ag_2O system into β-bronze crystallisation field in ternary system, etc., the eutectic points of binary system turn into eutectic lines in the ternary one.

The present paper deals with the molybdenum rich part of the ternary V_2O_5–MoO_3–Ag_2O system. Due to the appearance of previously unknown $AgVMoO_6$ ternary phase this part of the system is much more complicated than that vanadium rich. This necessitated constructing not only the section in which at constant vanadium/molybdenum molar ratio 3:7 the content of Ag_2O was varied, but also the sections of quasi-binary systems: β-$AgVO_3$–β-Ag_2MoO_4, $AgVMoO_6$–MoO_3, $AgVMoO_6$–$Ag_2Mo_4O_{13}$, $AgVMoO_6$–$Ag_2Mo_2O_7$, $AgVMoO_6$–β-Ag_2MoO_4 as it is shown by the scheme presented in Fig. 1. The study of the above sections of the ternary diagram aimed to control whether in this concentration region exist any other triple compounds (or phases) then the $AgVMoO_6$ phase and also to determine the limit of the crystallisation fields of the existing phases. The latter information has been used to determine the approximate positions of the double eutectic lines and triple points in the construction of ternary diagram which will be presented in the following publication [2].

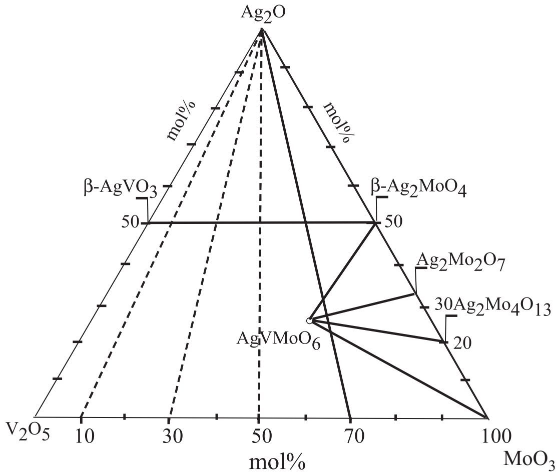

Fig. 1 Schematic representation of the quasi-binary subsystems in the V_2O_5–MoO_3–Ag_2O triple system investigated in the present (—) and in the previous (– –) research [1]. There are shown only the phases which were used to construct the quasi-binary subsystems presented in this paper

Experimental

The samples used for the construction of V_2O_5:MoO_3=3:7 cross section were obtained by sintering in different proportions the following oxides: V_2O_5 (‘Analar’, p.a.), MoO_3 (‘Reanal’, p.a.) and

---

* Author for correspondence: wenda@chemia.uj.edu.pl

1388–6150/$20.00

Akadémiai Kiadó, Budapest, Hungary
Springer, Dordrecht, The Netherlands

Table 1 Samples with V_2O_5 /MoO_3 molar ratio 3:7. Sintering conditions, phase composition and DTA analysis

Ag_2O/ mol%	Heating rate/ °C h^{-1}	Sintering temperature/°C	Time of the sintering/h	Average cooling rate/°C h^{-1}	Phase composition	Temperature of DTA endothermic effects/°C	Remarks
1	264	660	24	128	MoO_3, $V_9Mo_6O_{40}$ $AgVMoO_6$	565, 635, 670	Non pelleted
2	264	660	24	128	MoO_3, $V_9Mo_6O_{40}$ $AgVMoO_6$	570, 595, 665	–II–
5	264	660	24	128	MoO_3 , $V_9Mo_6O_{40}$ $AgVMoO_6$	575, 630, 655	–II–
10	264	660	24	128	MoO_3, $V_9Mo_6O_{40}$ $AgVMoO_6$	580	–II–
15	2.4	520	–	167	MoO_3 , $V_9Mo_6O_{40}$ $AgVMoO_6$	600	pellet
20	264	660	24	128	MoO_3, $V_9Mo_6O_{40}$ $AgVMoO_6$	570, 610	Non pelleted
25	10	520	–	167	$AgVMoO_6$ $Ag_2Mo_4O_{13}$, $Ag_2Mo_2O_7$	480, 490, 620	pellet
30	10	520	–	167	$AgVMoO_6$ β–Ag_2MoO_4 β– $AgVO_3$	430, 470, 605	pellet
35	8	400	–	128	$AgVMoO_6$ β–Ag_2MoO_4 β– $AgVO_3$	475, 585	pellet
40	8	400	–	128	$AgVMoO_6$ β–Ag_2MoO_4 β– $AgVO_3$	480, 535	pellet
45	380	400	48	128	$AgVMoO_6$ β–Ag_2MoO_4 β– $AgVO_3$	475	pellet
50	330	350	72	128	β–Ag_2MoO_4 β– $AgVO_3$	432, 490	pellet
55	330	350	72	128	β–$AgVO_3$, β–Ag_2MoO_4 Ag_3VO_4	360, 425	pellet
60	330	350	72	128	β–$AgVO_3$, β–Ag_2MoO_4 Ag_3VO_4	370, 405	pellet
65	330	350	72	128	β–Ag_2MoO_4 Ag_3VO_4 Ag	365	pellet
70	330	350	72	128	β–Ag_2MoO_4 Ag_3VO_4 Ag	365	pellet
75	330	350	72	128	β–Ag_2MoO_4 Ag_3VO_4 Ag	365, 375	pellet
80	380	400	48	128	β–Ag_2MoO_4 Ag_3VO_4 Ag	365, 400	pellet
85	as above	as above	as above	as above	β–Ag_2MoO_4 Ag_3VO_4 Ag	370	pellet
90	as above	as above	as above	as above	β–Ag_2MoO_4 Ag_3VO_4 Ag	445, 522	pellet

Ag_2O (POCh Gliwice, p.a.). Before each sintering the mixtures of the oxides were homogenised for 5 h in a pebble mill then pelleted and heated at temperatures which were never higher than 50°C below temperature of fusion. The sintered pellets were crushed and again homogenised, pelleted and sintered. The method of heating and cooling the samples was essentially the same as it was applied in a number of papers concerning metal oxide system, e.g. [5–8]. The conditions of all these operations are given in Table 1. The homogenisation-sintering cycles were repeated until then X-ray pattern and DTA curve no more changed. In the previous research it was observed that homogenisation longer than 24 h may result in the formation small amounts of the metallic silver. Hence in the present work we applied shorter homogenisation time (5 h) but increasing the number of homogenisation-sintering cycles. The behaviour of the mixtures (pelleted or not pelleted) was then controlled by DTG analysis. In the case of samples containing more than 15 mol% Ag_2O special care was necessary because of the possible decomposition of silver oxide above 440°C. Accordingly heat treatment of such samples was done at temperatures 350–400°C.

The following compounds: β-$AgVO_3$, β-Ag_2MoO_4, $AgVMoO_6$, $Ag_2Mo_4O_{13}$ and $Ag_2Mo_2O_7$ were prepared for construction of the other diagrams examined in this work.

β-$AgVO_3$ was obtained by heating the pelleted stoichiometric mixture of V_2O_5.and Ag_2O for 48 h at 370°C in the atmosphere of air. This temperature is the temperature of the exothermic DTA peak of the oxide mixture due to the reaction:

$$V_2O_5+Ag_2O=2\beta\text{-}AgVO_3 \qquad (1)$$

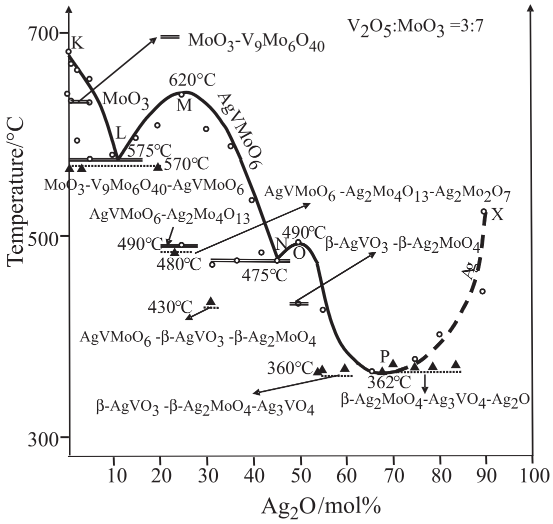

Fig. 2 V_2O_5:MoO_3=3:7 section of the ternary V_2O_5–MoO_3–Ag_2O diagram. ○ – temperatures of the endothermic effects on DTA curves; — – cross section of the (3:7) diagram plane with crystallization fields in the ternary system; === – cross section of double eutectic lines in ternary system with the (3:7) diagram plane; ▲ – temperature of ternary eutectic fusion points

X-ray phase analysis confirmed the presence of β-$AgVO_3$ as the only detectable phase.

β-Ag_2MoO_4 compound was obtained as α-form by precipitation from water solution:

$$Na_2MoO_4+AgNO_3=\alpha\text{-}Ag_2MoO_4+2NaNO_3 \qquad (2)$$

It was pressed into pellets and subsequently heated at 290°C i.e. some 10°C above the temperature of α→β transition. It was cooled down with average rate 5° min^{-1}. The presence of the β-form as the only phase was confirmed by X-ray diffraction.

Table 2 Binary system: β-$AgVO_3$–β-Ag_2MoO_4. Results of XRD and DTA analysis

No.	β-Ag_2MoO_4/ mol%	V_2O_5/MoO_3 molar ratio at 50 mol% Ag_2O	Phase composition	Temperature of DTA endothermic effects/°C
1	0[a]	-	β-$AgVO_3$	470
2	5.3[b]	90/10	β-$AgVO_3$, β-Ag_2MoO_4	480
3	17.6[b]	70/30	as above	430
4	33.3[b]	50/50	as above	430, 450
5	41[c]	40/60	β-$AgVO_3$, β-Ag_2MoO_4	400, 440
6	50[c]	33.3/66.7	as above	400, 425, 500
7	53.8[d]	30/70	as above	432, 460, 490
8	61[c]	24.2/75.8	as above	425, 510
9	65[c]	21.2/78.8	as above	425, 515
10	100[e]	-	β-Ag_2MoO_4	575

[a]data taken from [4]; [b]data taken from [1]; [c]the samples obtained by sintering of the β-$AgVO_3$–β-Ag_2MoO_4 mixtures. They were homogenised for 1 h in a pebble mill, pressed into pellets and then heated for 42 h at 340°C (samples 4 and 5), or at 415°C (samples 7 and 8). Next they were cooled down, analysed by X-ray, homogenised and heated 24 h at the same temperatures.; [d]data taken from Table 1 of the present work; [e]data taken from [3]

Table 3 Binary system: $AgVMoO_6$–MoO_3. Results of XRD and DTA analysis

MoO_3/ mol%	Phase composition	Temperature of DTA endothermic effects/°C
0[a]	$AgVMoO_6$	625
20[b]	$AgVMoO_6$, MoO_3	625
40[b]	MoO_3, $AgVMoO_6$	620, 610
60[b]	MoO_3, $AgVMoO_6$	611
80[b]	MoO_3, $AgVMoO_6$	612
100[c]	MoO_3	800

[a]data taken from [1]; [b]the samples obtained by sintering of $AgVMoO_6$–MoO_3 mixtures. They were homogenised for several hours in the pebble mill, pressed into pellets and then heated 48 h at 480°C. Next they were cooled down, analysed by X-ray, homogenised, pressed and heated 59 h at 500°C, cooled down 5 h.; [c]data taken from [3]

Table 4 Binary system: $AgVMoO_6$–$Ag_2Mo_4O_{13}$. Results of XRD and DTA analysis

$Ag_2Mo_4O_{13}$/ mol%	Phase composition	Temperature of DTA endothermic effects/°C
0[a]	$AgVMoO_6$	625
25[b]	$AgVMoO_6$, $Ag_2Mo_4O_{13}$	498, 526
37[b]	$AgVMoO_6$, $Ag_2Mo_4O_{13}$	497, 528
50[b]	$AgVMoO_6$, $Ag_2Mo_4O_{13}$	528
75[b]	$Ag_2Mo_4O_{13}$, $AgVMoO_6$	529
100[c]	$Ag_2Mo_4O_{13}$	536

[a]data taken from [1]; [b]the samples obtained by sintering of the $AgVMoO_6$, $Ag_2Mo_4O_{13}$ mixtures. They were homogenised for several hours in a pebble mill, pressed into pellets and then heated for 220 h at 400–450°C. Every 50–60 h the heating was interrupted, samples were cooled down, analysed by X-ray, homogenised, pressed and heated again.; [c]data taken from [3]

The details of $AgVMoO_6$ synthesis are given in [1] and those of $Ag_2Mo_4O_{13}$ as well as $Ag_2Mo_2O_7$ in [3]. The data concerning the sintering of particular samples forming quasi-binary systems including $AgVMoO_6$ phase are given in Tables 2–6.

Differential thermal analysis and X-ray diffraction phase analysis have been carried out and interpreted as described in [1]. In particular the temperature of the highest DTA peak was assumed to be the melting temperature of the sample. The DTA peaks at lower temperatures corresponded to the different effects depending on the sample composition. In particular they corresponded to the temperature of binary eutectic fusion (determined on Fig. 2 with double lines ==), and/or triple eutectic point (▲). In the case of the sample containing triple eutectic only one strong endothermic effect was observed.

Table 5 Binary system: $AgVMoO_6$–$Ag_2Mo_2O_7$. Results of XRD and DTA analysis

$Ag_2Mo_2O_7$/ mol%	Phase composition	Temperature of DTA endothermic effects/°C
0[a]	$AgVMoO_6$	625
24[b]	$AgVMoO_6$–$Ag_2Mo_2O_7$	479, 504
36[b]	$AgVMoO_6$–$Ag_2Mo_2O_7$	481, 506
50[b]	$AgVMoO_6$–$Ag_2Mo_2O_7$	482, 507
73[b]	$Ag_2Mo_2O_7$–$AgVMoO_6$	483, 508
100[c]	$Ag_2Mo_2O_7$	516

[a]data taken from [1]; [b]the samples obtained by sintering of the $AgVMoO_6$–$Ag_2Mo_2O_7$ mixtures. They were homogenised for several hours in a pebble mill, pressed into pellets and then heated for 250 h at 400–450°C. Every 50–60 h the heating was interrupted, samples were cooled down, analysed by X-ray, homogenised, pressed and heated again.; [c]data taken from [3]

Table 6 Binary system: $AgVMoO_6$–β-Ag_2MoO_4. Results of XRD and DTA analysis

β-Ag_2MoO_4/ mol%	Phase composition	Temperature of DTA endothermic effects/°C
0[a]	$AgVMoO_6$	625
15[b]	$AgVMoO_6$, β-Ag_2MoO_4	487, 617
32[b]	$AgVMoO_6$, β-Ag_2MoO_4	489, 599
51[b]	$AgVMoO_6$, β-Ag_2MoO_4	490
66[b]	β-Ag_2MoO_4, $AgVMoO_6$	490
83[b]	β-Ag_2MoO_4, $AgVMoO_6$	489, 532
100[c]	β-Ag_2MoO_4	574

[a]data taken from [1]; [b]the samples obtained by sintering of the $AgVMoO_6$, β-Ag_2MoO_4 mixtures. They were homogenised for several hours in a pebble mill, pressed into pellets and then heated for 72 h at 400–450°C. Every 10–15 h the heating was interrupted, samples were cooled down, analysed by X-ray, homogenised, pressed and heated again.; [c]data taken from [3]

Results and discussion

The V_2O_5:MoO_3= 3:7 cross section of the ternary diagram is shown in Fig. 2. The open circles show the temperatures of the highest DTA peak which–as already said – is assumed to determine melting temperature of the samples and, hence, liquidus line. The particular sections of the latter are laying on different crystallisation fields, those of MoO_3 (line KL), $AgVMoO_6$ (LMN), β-Ag_2MoO_4 (NOP) and Ag_2O (PX). Crystallisation fields of MoO_3 and $AgVMoO_6$ are separated by a line of double eutectic which cuts the plane of the diagram in Fig. 2 at point L. On lowering temperature the composition of the liquid changes along this double eutectic line and at 570°C reaches composition of a ternary eutectic point situated outside the diagram plane. In consequence the liquid samples of composition between that of point K and point L contain after solidification ternary eutectic MoO_3–$V_9Mo_6O_{40}$–$AgVMoO_6$ and possibly excess of MoO_3. Hence the X-ray analysis will show the presence MoO_3, $V_9Mo_6O_{40}$ and $AgVMoO_6$ phases in different proportions. The same phases are also present in the equilibrated samples obtained by sintering the oxides as it is shown in Table 1 for the samples with Ag_2O content 1–10 mol% and also 15 and 20 mol% Ag_2O. The two latter samples correspond to the melts of composition between L and M which on cooling separate $AgVMoO_6$, double eutectic $AgVMoO_6$–MoO_3 and the above mentioned triple eutectic. Sample containing 25 mol% Ag_2O exhibits the highest melting point (620°C) within this section of the diagram crossing crystallisation field of $AgVMoO_6$ phase (point M). The composition of the sample at this point is close to that of $AgVMoO_6$. On the Fig. 3 the DTA curve of this sample is shown.

In very much similar way can be explained the same qualitative phase composition of the samples between the compositions of points M and P. At still higher Ag_2O content we could not avoid decomposition of silver oxide and situation can not be simple interpreted.

The β-$AgVO_3$–β-Ag_2MoO_4 cross-section

The other cross-section of the ternary system the knowledge of which was important for the understanding of molybdenum rich part of this system was that along the line β-$AgVO_3$–β-Ag_2MoO_4 (Fig. 1). In this cross-section the content of Ag_2O was constant and equal to 50 mol% but vanadium–molybdenum ratio was changing within wide limits. The data concerning the chemical and phase compositions as well as temperatures of endothermic effects are given in Table 2.

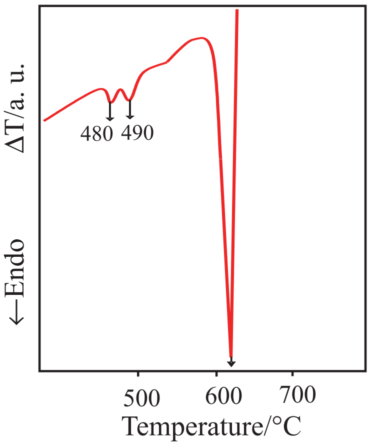

Fig. 3 DTA curve of sample with 25 mol% Ag_2O in V_2O_5:MoO_3=3:7 section

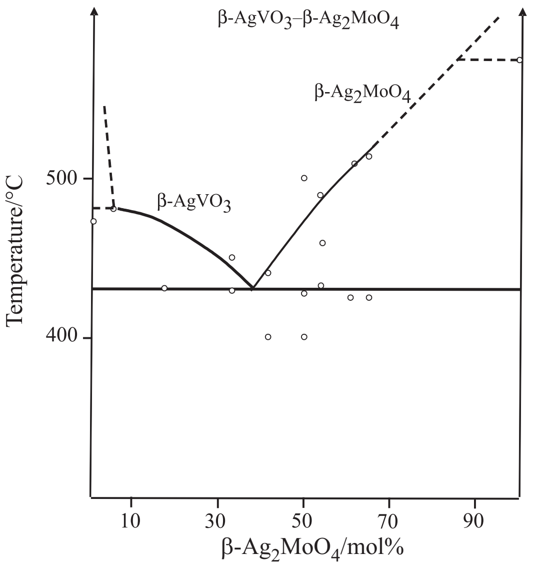

Fig. 4 The phase diagram of binary β-$AgVO_3$–β-Ag_2MoO_4 system

Figure 4 shows that compounds β-$AgVO_3$ and β-Ag_2MoO_4 are forming simple eutectic system with eutectic point at 430°C. In ternary system this point is situated on the line along which the crystallisation fields of β-$AgVO_3$ and β-Ag_2MoO_4 intersect. This section of the diagram has been constructed to obtain information concerning the region containing about 50 mol% Ag_2O which are needed for the construction of ternary diagram and in particular to obtain the position of the line along which crystallisation fields of β-$AgVO_3$ and β-Ag_2MoO_4 intersect. However, both compounds are melting incongruently and this fact has been shown on the diagram (Fig. 4) only schematically by the dotted lines.

The $AgVMoO_6$–MoO_3, $AgVMoO_6$–$Ag_2Mo_4O_{13}$, $AgVMoO_6$–$Ag_2Mo_2O_7$ and $AgVMoO_6$–β-Ag_2MoO_4 cross sections

The full understanding of the phase equilibriums in the molybdenum rich area of the triple diagram needed construction of the double component sections mentioned above. Considering the fact already mentioned that molybdenum oxide sublimes below its melting point (e.g. 800°C) and silver oxide decomposes above 440°C the samples for the investigation of the quasi-binary systems were obtained not from simple oxides but using independently prepared compounds $Ag_2Mo_4O_{13}$, $AgVMoO_6$, $Ag_2Mo_2O_7$ and β-Ag_2MoO_4 which are thermally much more stable.

All the above mentioned binary systems appeared to be simple eutectic systems of the compounds which, with the exception of β-Ag_2MoO_4, are

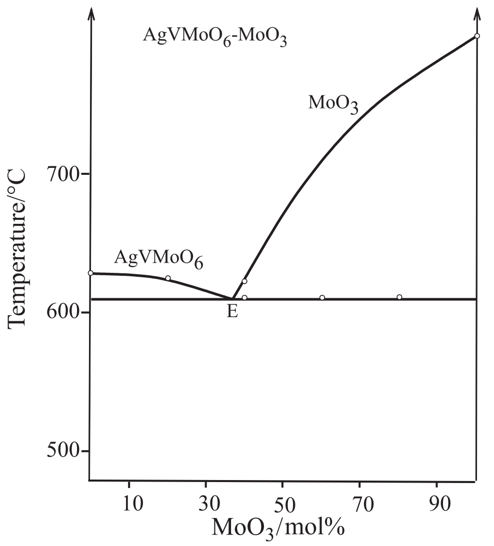

Fig. 5 The phase diagram of binary $AgVMoO_6$–MoO_3 system

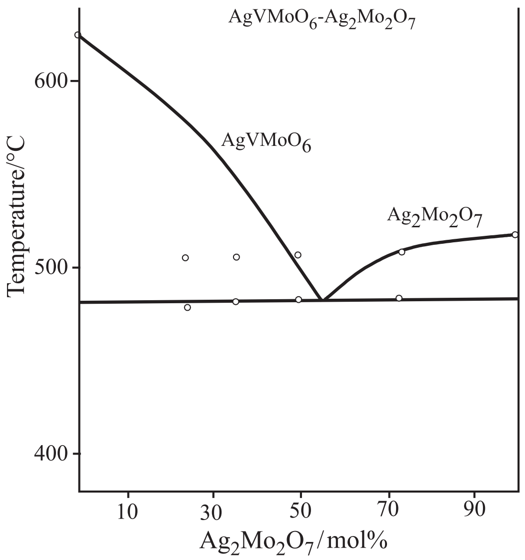

Fig. 7 The phase diagram of binary $AgVMoO_6$–$Ag_2Mo_2O_7$ system

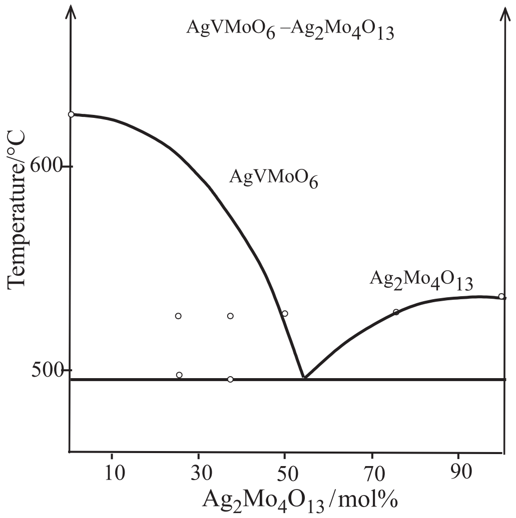

Fig. 6 The phase diagram of binary $AgVMoO_6$–$Ag_2Mo_4O_{13}$ system

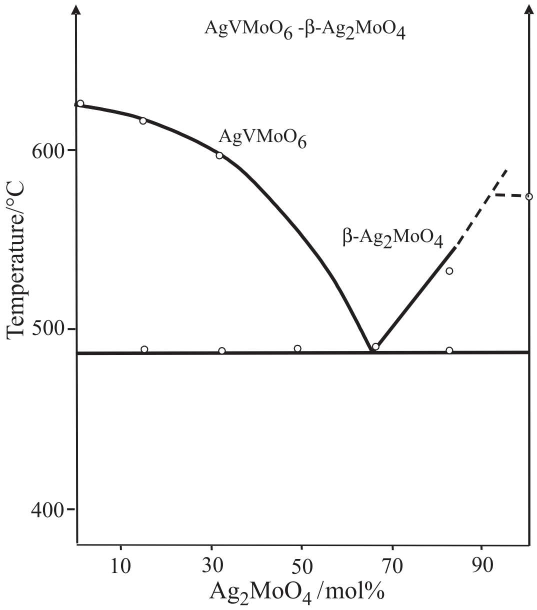

Fig. 8 The phase diagram of binary $AgVMoO_6$–β-Ag_2MoO_4 system

congruently melting. The points of the double eutectics are situated on the lines along which the crystallisation field of $AgVMoO_6$ crosses with those of MoO_3, $Ag_2Mo_4O_{13}$, $Ag_2Mo_2O_7$ or β-Ag_2MoO_4. The data concerning the preparation of the samples and rantgenographically detected phases are collected in Tables 3–6. Prolonged periods of sintering and cooling were applied. The heating-cooling cycles were repeated several times. It has been stated that no other ternary compounds besides $AgVMoO_6$ phase are forming in the investigated part of the ternary system.

The diagram of the binary system $AgVMoO_6$–MoO_3 is presented in Fig. 5 and the pertaining data are in Table 3. Both congruently melting compounds are forming eutectic at 37 mol% MoO_3 melting at 611°C (point E). Analogous information concerning the binary systems:

$AgVMoO_6$–$Ag_2Mo_4O_{13}$
(eutectic at 54 mol% $Ag_2Mo_4O_{13}$ melting at 497°C),
Fig. 6, Table 4

$AgVMoO_6$–$Ag_2Mo_2O_7$
(eutectic at 56 mol% $Ag_2Mo_2O_7$, melting at 483°C)
Fig. 7, Table 5

$AgVMoO_6$–β-Ag_2MoO_4
(eutectic at 63 mol% β-Ag_2MoO_4, melting at 489°C)
Fig. 8, Table 6

Conclusions

The paper presents the results of the investigation of the molybdenum oxide rich part of the ternary system V_2O_5–MoO_3–Ag_2O. In particular the cross section of ternary diagram was studied in which V_2O_5/MoO_3 molar ratio was constant and equal to 3:7 but the concentration of Ag_2O was variable. This was the supplemented by the determination of four quasi-binary systems including the new phase $AgVMoO_6$, presumably the compound, and MoO_3, $Ag_2Mo_4O_{13}$, $Ag_2Mo_2O_7$ as well as β-Ag_2MoO_4. The paper presents also quasi-binary system β-$AgVO_3$–β-Ag_2MoO_4. All the data presented in this paper and also the earlier papers [1–3] will be used to construct full ternary diagram V_2O_5–MoO_3-Ag_2O which will be object of the following paper [2].

References

1 E. Wenda and A. Bielański, J. Therm. Anal. Cal., DOI: 10.1007/s10973-007-8339-6.
2 E. Wenda and A. Bielański, J. Therm. Anal. Cal., DOI: 10.1007/s10973-007-8341-z.
3 E. Wenda, J. Thermal Anal., 36 (1990) 1417.
4 E. Wenda, J.Thermal Anal., 30 (1985) 879.
5 A. Blonska-Tabero and M. Kurzawa, J. Therm. Anal. Cal., 88 (2007) 33.
6 P. Tabero, J. Therm. Anal. Cal., 88 (2007) 37.
7 M. Bosacka, J. Therm. Anal. Cal., 88 (2007) 43.
8 A. Blonska-Tabero, J. Therm. Anal. Cal., 88 (2007) 201.

Received: January 15, 2007
Accepted: November 6, 2007

DOI: 10.1007/s10973-007-8340-0